The CPEB3 ribozyme modulates hippocampal-dependent memory

Claire C. Chen[1], Joseph Han[2], Carlene A. Chinn[2], Xiang Li[2†], Mehran Nikan[3], Marie Myszka[4], Liqi Tong[5], Timothy W. Bredy[2†], Marcelo A. Wood[2*], Andrej Lupták[1,4,6*]

[1] Department of Pharmaceutical Sciences, University of California–Irvine, Irvine, California 92697, United States.

[2] Department of Neurobiology and Behavior, Center for the Neurobiology of Learning and Memory, University of California–Irvine, Irvine, California 92697, United States.

[3] Ionis Pharmaceuticals, 2855 Gazelle Court, Carlsbad, CA 92010, USA.

[4] Department of Chemistry, University of California–Irvine, Irvine, California 92697, United States.

[5] Institute for Memory Impairments and Neurological Disorders, University of California–Irvine, Irvine, California 92697, United States.

[6] Department of Molecular Biology and Biochemistry, University of California–Irvine, Irvine, California 92697, United States

*Correspondence to: Andrej Lupták. Department of Pharmaceutical Sciences, University of California–Irvine, Irvine, California 92697, United States. aluptak@uci.edu. Marcelo A. Wood. Department of Neurobiology and Behavior, Center for the Neurobiology of Learning and Memory, University of California–Irvine, Irvine, California 92697, United States. mwood@uci.edu.

[†] Present address: Cognitive Neuroepigenetics Laboratory, Queensland Brain Institute, The University of Queensland, Brisbane, QLD 4072, Australia.

Keywords: ribozyme, splicing, self-scission, polyadenylation, local translation

Abstract

A self-cleaving ribozyme mapping to an intron of the cytoplasmic polyadenylation element binding protein 3 (CPEB3) gene has been suggested to play a role in human episodic memory, but the underlying mechanisms mediating this effect are not known. The ribozymes maps to the second intron of the *CPEB3* gene and its self-scission half-life matches the time it takes an RNA polymerase to reach the immediate downstream exon, suggesting that the ribozyme-dependent intron cleavage is tuned to co-transcriptional splicing of the *CPEB3* mRNA. Here we report that the murine ribozyme modulates its own host mRNA maturation in both cultured cortical neurons and the hippocampus. Inhibition of the ribozyme using an antisense oligonucleotide leads to increased CPEB3 protein expression, which enhances polyadenylation and translation of localized plasticity-related target mRNAs, and subsequently strengthens hippocampal-dependent long-term memory. These findings reveal a previously unknown role for self-cleaving ribozyme activity in regulating experience-induced co-transcriptional and local translational processes required for learning and memory.

Introduction

Cytoplasmic polyadenylation element binding proteins (CPEBs) are RNA-binding proteins that modulate polyadenylation-induced mRNA translation, which is essential for the persistence of memory (Huang et al., 2003). CPEBs have been found in several invertebrate and vertebrate genomes, and four *CPEB* genes (*CPEB1–4*) have been identified in mammals (Richter, 2007; Si et al., 2003; Theis et al., 2003). All CPEB proteins have two RNA recognition domain (RRM motifs) and two zinc-finger motifs in the C-terminal region, but differ in their N-terminal domains (Hake and Richter, 1994; Huang et al., 2006; Ivshina et al., 2014). *Aplysia* CPEB (ApCPEB), *Drosophil*a Orb2, and mouse CPEB3 have two distinct functional conformations that correspond to soluble monomers and amyloidogenic oligomers, and have been implicated in maintenance of long-term facilitation (LTF) in *Aplysia* and long-term memory in both *Drosophil*a and mice (Fioriti et al., 2015; Hervas et al., 2016; Hervas et al., 2020; Majumdar et al., 2012; Miniaci et al., 2008; Rayman and Kandel, 2017; Si et al., 2010). In *Drosophil*a, inhibition of amyloid-like oligomerization of Orb2 impairs the persistence of long-lasting memory, and deletion of prion-like domain of Orb2 disrupts long-term courtship memory (Hervas et al., 2016; Keleman et al., 2007). The aggregated form of CPEB3, which is inhibited by SUMOylation, can mediate target mRNA translation at activated synapses (Drisaldi et al., 2015).

Following synaptic stimulation CPEB3 interacts with actin cytoskeleton, with a positive feedback loop of CPEB3/actin regulating remodeling of synaptic structure and connections (Gu et al., 2020; Stephan et al., 2015). Studies of CPEB3 in memory

formation revealed that the local protein synthesis and long-term memory storage are regulated by the prion-like CPEB3 aggregates (the aggregation of CPEB3 is thought to strengthen synaptic plasticity in the hippocampus); *CPEB3* conditional knockout mice display impairments in memory consolidation, object placement recognition, and long-term memory maintenance (Fioriti et al., 2015). On the other hand, global *CPEB3* knockout mice display enhanced spatial memory consolidation in the Morris water maze and exhibit elevated short-term fear during the acquisition and extinction of contextual fear memory (Chao et al., 2013).

An *in vitro* selection from a human-genome-derived library has revealed a mammalian-conserved self-cleaving ribozyme in the second intron of the *CPEB3* gene (Salehi-Ashtiani et al., 2006; Webb and Luptak, 2011) (Figure 1A). The ribozyme shares its secondary structure and catalytic mechanism with the hepatitis delta virus (HDV) ribozyme (Skilandat et al., 2016; Webb and Luptak, 2011). In humans, a single nucleotide polymorphism (SNP) at the ribozyme cleavage site leads to a 3-fold higher rate of *in vitro* self-scission, which correlates with poorer performance in an episodic memory task (Salehi-Ashtiani et al., 2006; Vogler et al., 2009). These findings suggested that the ribozyme activity might play a role in memory formation. Given that the self-scission of intronic ribozymes is inversely correlated with splicing efficiency of the harboring pre-mRNA (Fong et al., 2009), we hypothesized that modulation of the CPEB3 ribozyme can alter *CPEB3* mRNA splicing and increase the expression of full-length mRNA and protein. This would lead to the polyadenylation of its target mRNAs and an enhancement in the consolidation of hippocampal-dependent memory.

Results

CPEB3 mRNA expression and ribozyme activity are upregulated in response to neuronal stimulation.

To test this hypothesis, we began by measuring the co-transcriptional self-scission of the murine variant of the ribozyme *in vitro* and found a half-life ($t_{1/2}$) of ~2 minutes (Figure 1B and Table S1), which is similar to previously measured chimp and fast-reacting human variants of the ribozyme (Chadalavada et al., 2010). Because the distance from the ribozyme to the 3rd exon in the *CPEB3* gene is about 10 kb and the RNA polymerase II (RNAPII) transcription rate of long mammalian genes is estimated to be ~3.5–4.1 knt/min (Singh and Padgett, 2009), RNAPII would take about 2.5–3 minutes to reach the 3rd exon and mark it for splicing. This result suggested that the ribozyme activity is tuned to the co-transcriptional processing of the CPEB3 pre-mRNA.

The neuronal activity-dependent gene regulation is essential for synaptic plasticity (Neves et al., 2008). To investigate the effect of the CPEB3 ribozyme on *CPEB3* mRNA expression and measure its effect on maturation and protein levels, primary cortical neurons were stimulated by glutamate or potassium chloride (KCl). First, *CPEB3* mRNA levels were measured using primers that specifically amplified exon–exon splice junctions (Exons 2–3, 3–6, 6–9; Figure 1A). We found that membrane depolarization by KCl led to an up-regulation of *CPEB3* mRNA 2 hours post stimulation, compared with non-stimulated cultures (Figure 1C). To examine CPEB3 ribozyme activity, total ribozyme and uncleaved ribozyme levels were measured by qRT-PCR, which showed that ribozyme expression is elevated at 1 hour following KCl treatment (Figure 1D).

Similarly, glutamate stimulation both increased the expression of spliced exons by 2–3 fold at 2 hours, with a decrease observed at later time points (Figure 1E), and increased ribozyme expression correlated with CPEB3 mRNA expression (Figure 1F). This finding is supported by previous studies showing that synaptic stimulation by glutamate leads to an increase in CPEB3 protein expression in hippocampal neurons (Fioriti et al., 2015) and that treatment with kainate likewise induces CPEB3 expression in the hippocampus (Theis et al., 2003). The cleaved fraction of the ribozyme was greatest at the highest point of CPEB3 mRNA expression, suggesting efficient co-transcriptional self-scission. Together, these data (i) indicate that the self-cleaving CPEB3 ribozyme is expressed, and potentially activated, in response to neuronal activity, and (ii) suggest that CPEB3 ribozyme *cis*-regulates the maturation of CPEB3 mRNA.

CPEB3 mRNA and protein levels increase in primary neuronal cultures treated with ribozyme inhibitor.

Because our data showed that CPEB3 ribozyme expression is correlated with mRNA expression, we hypothesized that regulation of the ribozyme may modulate CPEB3 mRNA splicing. To test this hypothesis, we inhibited the ribozyme using antisense oligonucleotides (ASOs) spanning the cleavage site (Figures 2A and 2B); these ASOs were similar to those previously used to inhibit *in vitro* co-transcriptional self-scission of this family of ribozymes (Harris et al., 2004; Webb et al., 2009). ASOs are synthetic single-stranded nucleic acids that can bind to pre-mRNA or mature RNA through base-pairing, and typically trigger RNA degradation by RNase H, thereby turning off the target gene expression. ASOs have also been used to modulate alternative splicing,

suggesting that they act co-transcriptionally (e.g., to correct *SMN2* gene) (Hua et al., 2010). The ASOs used in this study were designed to increase thermal stability of complementary hybridization and, as a result, to induce higher binding affinity for the ribozyme.

To study the effect of the CPEB3 ribozyme on *CPEB3* mRNA expression, neuronal cultures were pretreated with either an ASO or a non-targeting control oligonucleotide, followed by KCl stimulation. In the absence of ASO, KCl induced a rapid and robust increase in ribozyme levels compared to cultures containing scrambled ASO, and this effect was suppressed in the presence of ASO, suggesting that the ribozyme is blocked by the ASO within 2 hours of induction (Figure S1A). At an early time point (2 hours post-KCl induction), the ASO-containing culture displayed an increase of spliced mRNA (Figures 2C, S1 B and C), suggesting that the ASO prevents CPEB3 ribozyme from cleaving the intron co-transcriptionally and promotes mRNA maturation. At 24 hours post-KCl induction, however, there was no significant difference in CPEB3 ribozyme expression among groups (Figure S1D). Likewise, the level of *CPEB3* mRNA exons 2–3 returned to the basal level (Figure S1E), while exons 3–6 remained slightly elevated in the ASO-treatment groups (Figure S1F). The mRNA expression of CPEB3 exons 6–9 remained stable over time and was not affected by ASO treatment or KCl stimulation (Figure S1G). Taken together, these data suggest that the CPEB3 ribozyme modulates the production of the full-length *CPEB3* mRNA.

To evaluate whether the ASO specifically targets CPEB3 ribozyme or modulates intron levels in general, we measured the levels of the 4th CPEB3 intron, which does not harbor a self-cleaving ribozyme. No significant difference in the 4th intron expression between groups was observed, demonstrating that the ASO does not have a broad non-specific effect on the stability of other introns (Figure S2H). Furthermore, to assess whether the ASO induces cytotoxicity *in vitro*, neuronal cultures were treated with either ASO or scrambled ASO. Cell viability was measured with an XTT assay, revealing no difference in either ASO- or scrambled ASO-treated cells, compared to untreated cells. These data suggest that the ASOs used in this study did not induce cytotoxic effects in cultured neurons (Figure S1I).

We next determined whether inhibition of CPEB3 ribozyme regulates CPEB3 protein expression. Treatment with the ribozyme ASO resulted in a significant increase in CPEB3 protein levels in both the basal state and under KCl-stimulated conditions, indicating a coordination of activity-dependent transcription and translation upon inhibition of CPEB3 ribozyme activity (Figure 2D).

Ribozyme inhibition leads to increased expression of plasticity-related proteins.

In *Aplysia* sensory-motor neuron co-culture, application of repeated pulses of serotonin (5-HT) induces ApCPEB protein expression at the stimulated synapses and LTF, which is a form of learning-related synaptic plasticity that is widely studied in *Aplysia* (Si et al., 2010; Si et al., 2003). In murine primary hippocampal neurons, the level of CPEB3 protein expression is positively regulated by neuronal activity (Fioriti et al., 2015) and

plays dual roles in regulating mRNA translation (Du and Richter, 2005; Stephan et al., 2015) whereby a post-translational modification of CPEB3 can convert it from a repressor to an activator: a monoubiquitination by Neuralized1 leads to activation of CPEB3, which promotes subsequent polyadenylation and translation of GluA1 and GluA2 (Pavlopoulos et al., 2011). Previous studies have also demonstrated the role of CPEB3 in the translational regulation of a number of plasticity-related proteins (PRPs), including AMPA-type glutamate receptors (AMPARs), NMDA receptor (NMDAR), and postsynaptic density protein 95 (PSD-95) (Chao et al., 2012; Chao et al., 2013; Fioriti et al., 2015; Huang et al., 2006). As an RNA binding protein, CPEB3 has been shown to bind to 3′ UTR of GluA1, GluA2, and *PSD-95* mRNAs and to regulate their polyadenylation and translation (Chao et al., 2013; Fioriti et al., 2015; Huang et al., 2006; Pavlopoulos et al., 2011).

To test whether inhibition of CPEB3 ribozyme modulates expression of PRPs, we measured the protein levels by immunoblotting. We found that under KCl-induced depolarizing conditions, treatment with the CPEB3 ribozyme ASO resulted in a significant increase in GluA1 and PSD-95 protein expression, whereas GluA2 levels remained unchanged (Figures S2, A and B). Likewise, ASO treatment led to an up-regulation of NR2B protein, one of the NMDAR subunits (Figures S2, C and D). These results suggest that CPEB3 ribozyme activity affects several downstream processes, particularly mRNA maturation and translation, as well as the expression of PRPs, including the translation of AMPAR and NMDAR mRNAs.

CPEB3 ribozyme ASO leads to an increase of CPEB3 mRNA and polyadenylation of PRPs in the CA1 hippocampus.

To investigate whether the CPEB3 ribozyme exhibits similar effects in regulating genes related to synaptic plasticity *in vivo*, mice were stereotaxically infused with either ribozyme ASO, scrambled ASO, or vehicle into the CA1 region of the dorsal hippocampus, a major brain region involved in memory consolidation and persistence (Figure 3A). Infusion of ASO targeting the CPEB3 ribozyme significantly reduced ribozyme levels detected by RT-qPCR in the dorsal hippocampus (Figure S3A). We found that administration of ASO led to an increase of *CPEB3* mRNA in the CA1 hippocampus (Figure 3B), confirming that the ASO prevents ribozyme self-scission during CPEB3 pre-mRNA transcription, thereby increasing *CPEB3* mRNA levels. No significant difference in the 4th intron levels was observed between ASO and vehicle (Figure S3B). Next, immunoblotting was used to determine whether the CPEB3 ribozyme inhibition affects CPEB3 translation, and no significant difference between ASO and control groups was observed (Figures S5, A and B). We observed that blocking the CPEB3 ribozyme does not change GluA1, GluA2, PSD-95, and NR2B mRNA or protein expression in naïve mice (Figures S4, S5A and S5C). Thus, in naïve mice, ribozyme inhibition leads to increased basal levels of the *CPEB3* mRNA, but the levels of the CPEB3 protein and its downstream targets remain unchanged.

To further delineate whether the CPEB3 ribozyme activity results in polyadenylation of downstream mRNAs, 3′ rapid amplification of cDNA ends (3′ RACE) was performed to examine the 3′ termini of several mRNAs. We found that ribozyme ASO administration

led to increased GluA1, GluA2, and PSD-95 mRNA polyadenylation in the mouse dorsal hippocampus (Figure 3C). These data support a model wherein the inhibition of the CPEB3 ribozyme leads to increased polyadenylation of existing AMPARs and PSD-95 mRNAs, and suggests a role in post-transcriptional regulation and 3′ mRNA processing.

Inhibition of CPEB3 ribozyme in the dorsal hippocampus enhances long-term memory.

To assess whether inhibition of the CPEB3 ribozyme improves memory formation, we examined the CPEB3 ribozyme with respect to long-term memory using the object location memory (OLM) task (Figure 4A). The OLM task has been widely used to study hippocampal-dependent spatial memory. The task is based on an animal's innate preference for novelty and its capability for discriminating spatial relationships between novel and familiar locations (Vogel-Ciernia and Wood, 2014). During a testing session, mice retrieve the memory that encoded for the objects they were exposed to in the training session. We infused mice bilaterally into the CA1 dorsal hippocampus with the CPEB3 ribozyme ASO, scrambled ASO, or vehicle 48 hours prior to OLM training. The CPEB3 ribozyme ASO group showed a significant increase in discrimination index (DI) between training and testing compared to control groups, suggesting that these mice experienced a robust enhancement of novel object exploration (Figure 4B). We observed no significant difference in training DI ($P > 0.05$), indicating that mice exhibit no preference for either object (Figure 4B). Likewise, during training and testing sessions, ASO-infused mice and control mice displayed similar total exploration time, demonstrating that both groups of mice have similar exploitative behavior (Figure 4C).

These results provide strong evidence that CPEB3 is critical for long-term memory, and that the CPEB3 ribozyme activity in particular is necessary for the formation of long-term memory.

CPEB3 ribozyme ASO leads to an upregulation in protein expression of CPEB3 and PRPs during memory consolidation.

Learning-induced changes in gene expression and protein synthesis are essential for memory formation and consolidation (Kandel, 2001). To determine whether upregulation of CPEB3 mRNA by the ribozyme ASO leads to a change in expression of the CPEB3 protein and its downstream targets, we analyzed the dorsal hippocampal homogenates and synaptosomal fractions. Administration of CPEB3 ribozyme ASO led to a significant increase of CPEB3 protein expression in the CA1 hippocampal homogenates and crude synaptosomes 1 hour after OLM testing (Figures 5, A, B, and D). This result confirms that ASO-mediated knockdown of the CPEB3 ribozyme facilitates CPEB3 mRNA processing and translation. The protein expression of GluA1, GluA2, PSD-95, and NR2B were measured to determine whether increased CPEB3 further regulates translation of PRPs. In total tissue lysates, no significant difference in PRPs levels was observed between ASO and control (Figures 5, A and C). However, in synaptosomal fractions, GluA1, PSD-95, and NR2B protein expression levels were elevated in ASO-infused mice relative to scrambled ASO control animals; GluA2 protein level remained unaffected (Figures 5, A and E). Our findings indicate that blocking CPEB3 ribozyme activity leads to an increase in CPEB3 protein production, and up-

regulation of CPEB3 by OLM further mediates local GluA1, PSD-95, and NR2B translation.

Discussion

Self-cleaving ribozymes are broadly distributed small functional RNAs that catalyze a site-specific scission of their backbone (Jimenez et al., 2015). The HDV family of these ribozymes act during rolling circle replication of the HDV RNA genome and in processing of retrotransposons (Eickbush and Eickbush, 2010; Ruminski et al., 2011; Sanchez-Luque et al., 2011; Sharmeen et al., 1988; Wu et al., 1989), but given their distribution in nature, their biological roles are largely unexplored. Mammals harbor several self-cleaving ribozymes with unknown biological functions (de la Pena and Garcia-Robles, 2010; Martick et al., 2008; Salehi-Ashtiani et al., 2006). One of these ribozymes, the HDV-like CPEB3 ribozyme, maps to the second intron of the *CPEB3* gene and its *in vitro* activity (Figures 1A and 1B) suggested that its rate of self-scission may be tuned to disrupt the intron at a rate that is similar to the production speed of the downstream intronic sequence ahead of the next exon. Previous work on synthetic ribozymes placed within introns of mammalian genes showed that splicing of the surrounding exons is sensitive to the continuity of the intron: fast ribozymes caused efficient self-scission of the intron, leading to unspliced mRNA and resulting in lower protein expression, whereas slow ribozymes had no effect on mRNA splicing and subsequent protein expression (Fong et al., 2009). Inspired by this work, we investigated how the intronic ribozyme affects the *CPEB3* mRNA maturation and translation, and its subsequent effect on memory formation in mice.

Modifications of synaptic strength are thought to underlie learning and memory in the brain. Studies in hippocampal slices revealed that local translation in dendrites has been observed following induction of LTP (Frey and Morris, 1997). Cytoplasmic polyadenylation-induced translation is one of the key steps for regulating protein synthesis and neuroplasticity (Du and Richter, 2005; Richter, 2007, 2010). One of the proteins involved in regulation of cytoplasmic polyadenylation of mRNAs is CPEB3. Recent studies have shown that CPEB3 regulates mRNA translation of several PRPs at synapses, where it is essential for synaptic strength (Fioriti et al., 2015; Huang et al., 2006; Pavlopoulos et al., 2011). Previous reports have shown that CPEB3 regulates GluA1 and GluA2 polyadenylation: CPEB3 conditional knockout mice fail to elongate the poly(A) tail of GluA1 and GluA2 mRNA after Morris water maze training, and overexpression of CPEB3 changes the length of the GluA1 and GluA2 mRNA poly(A) tail (Fioriti et al., 2015). Because translational control by regulation of CPEB3 has been demonstrated to contribute to the hippocampal-dependent learning and memory (Pavlopoulos et al., 2011), one unaddressed question is whether the CPEB3 expression is modulated by the CPEB3 ribozyme. In mammals, the coordination of pre-mRNA processing and transcription can affect its gene expression (Neugebauer, 2019). Recent measurement of co-transcriptional splicing events in mammalian cells using long-read sequencing and Precision Run-On sequencing (PRO-seq) approaches demonstrated that co-transcriptional splicing efficiency impacts productive gene output (Reimer et al., 2020). The temporal and spatial window shows that the splicing and transcription machinery are tightly coupled. In agreement with this co-transcriptional splicing model,

our study shows that inhibition of the intronic CPEB3 ribozyme leads to an increase in CPEB3 mRNA and protein levels in primary cortical neurons and the dorsal hippocampus upon synaptic stimulation, and leading to changes in polyadenylation of target mRNAs of the CPEB3 protein.

Activity-dependent synaptic changes are governed by AMPAR trafficking, and AMPARs are mobilized to the post-synaptic surface membrane in response to neuronal activity in a dynamic process (Diering and Huganir, 2018). Our data demonstrate that the activation of CPEB3 by neuronal stimulation further facilitates translation of PRPs *in vivo*. These observations are consistent with a model in which learning induces CPEB3 protein expression, and ablation of CPEB3 abolishes the activity-dependent translation of GluA1 and GluA2 in the mouse hippocampus (Fioriti et al., 2015). Specifically, it has been suggested that CPEB3 converts to prion-like aggregates in stimulated synapses that mediate hippocampal synaptic plasticity and facilitate memory storage (Si and Kandel, 2016). Long-term memory formation is dependent on transcriptional and translational regulation. Because training can produce effective long-term memory, it is likely that CPEB3 ribozyme inhibition leads to increased CPEB3 protein expression and further facilitates experience-induced local translational processes.

In summary, we have delineated an important step in molecular mechanisms underlying a unique role for the CPEB3 ribozyme in post-transcriptional maturation of CPEB3 mRNA and its subsequent translation in mouse CA1 hippocampus. Modulation of CPEB3 ribozyme by ASO and OLM training induce activity-dependent upregulation of

CPEB3 and local production of PRPs. These molecular changes are critical for establishing persistent changes in synaptic plasticity that are required for long-term memory, and represent a novel biological role for activity-inducible self-cleaving ribozymes in the brain. More broadly, our study demonstrates a novel biological role for self-cleaving ribozymes and the first example of their function in mammals.

Materials and Methods

Primary cortical neuronal culture

Pregnant female C57BL/6 mice (The Jackson Laboratory) were euthanized at E18, and embryos were collected into an ice-cold Neurobasal medium (Thermo Fisher Scientific). Embryonic cortices were dissected, meninges were removed, and tissues were minced. Cells were mechanically dissociated, passed through a 40-μm cell strainer, counted, and plated at a density of 0.5 x 10^6 cells per well in six-well plates coated with poly-D-lysine (Sigma-Aldrich). Neuronal cultures were maintained at 37 °C with 5% CO_2, and grown in Neurobasal medium containing 2% B27 supplement (Thermo Fisher Scientific), 1% penicillin/streptomycin (Thermo Fisher Scientific), and 2 mM L-Glutamine (Thermo Fisher Scientific) for 7–10 days *in vitro* (DIV), with 50% of the medium being replaced every 3 days. All experimental procedures were performed according to the National Institutes of Health Guide for the Care and Use of Laboratory Animals and approved by the Institutional Animal Care and Use Committee of the University of California, Irvine.

Mice

C57BL/6J mice (8–10 weeks old, The Jackson Laboratory) were housed in a 12-h light/dark cycle and had free access to water and food. All experiments were conducted during the light cycle. All experimental procedures were performed according to the National Institutes of Health Guide for the Care and Use of Laboratory Animals and approved by the Institutional Animal Care and Use Committee of the University of California, Irvine.

Measurement of co-transcriptional self-scission of the CPEB3 ribozyme

Transcription reactions were set up in a 5-μL volume and incubated for 10 minutes at 25 ºC, as described previously (Passalacqua et al., 2017). The reactions contained: 1 μL of 5x transcription buffer (10 mM spermidine, 50 mM dithiothreitol, 120 mM Tris chloride buffer, pH 7.5, and 0.05% Triton X-100), 1 μL of 5x ribonucleoside triphosphates (final concentration of 6.8 mM), 1 μL of 5 mM Mg^{2+}, 1 μL DNA amplified by PCR to about 1 μM final concentration, 0.5 μL of 100% DMSO, 0.15 μL of water, 0.1 μL of murine RNase inhibitor (40,000 units/mL, New England Biolabs), 0.125 μL of T7 polymerase, and 0.125 μL [α-^{32}P]ATP. To prevent initiation of new transcription, the reactions were diluted into 100 μL of physiological-like buffer solution at 37 ºC. The solution consisted of 2 mM Mg^{2+} (to promote ribozyme self-scission), 140 mM KCl, 10 mM NaCl, and 50 mM Tris chloride buffer (pH 7.5). The 100-μL solution was then held at 37 ºC for the reminder of the experiment while aliquots were withdrawn at various time points. An equal volume of 4 mM EDTA/7 M urea stopping solution was added to each aliquot collected. Aliquots were resolved using denaturing polyacrylamide gel electrophoresis (PAGE, 7.5% polyacrylamide, 7 M urea) at 20 W. The PAGE gel was exposed to a phosphosimage screen for ~2 hours and analyzed using a Amersham Typhoon imaging system (GE Healthcare). Band intensities corresponding to the uncleaved ribozymes and the two products of self-scission were analyzed using ImageQuant (GE Healthcare) and exported into Excel. Fraction Intact was calculated as the intensity of the band corresponding to the uncleaved ribozyme divided by the sum of band intensities in a given PAGE lane. The data were fit to a biexponential decay model:

$k_{obs} = A \times e^{-k(1)t} + B \times e^{-k(2)t} + C$

In the case of the minimum murine CPEB3 ribozyme construct (-10/72; fig S2 and table S1), the data were modeled by a monoexponential decay with an uncleaved fraction (using parameters A, k_1, and C only).

Antisense oligonucleotides (ASOs)

ASOs used in this study are 20 nucleotides in length and are chemically modified with 2′-*O*-methoxyethyl (MOE, underlined) and 2′-4′ constrained ethyl (cEt, bold) (Seth et al., 2009). All internucleoside linkages are modified with phosphorothioate linkages to improve nuclease resistance. ASOs were solubilized in sterile phosphate-buffered saline (PBS). The sequences of the ASOs are as follows (all cytosine nucleobases are 5-methyl substituted):

Scrambled control ASO: 5′-**C**CT**T**CC**C**TG**A**AG**G**TTCCT**C**C-3′;

CPEB3 ribozyme ASO: 5′-**T**GT**G**GC**C**CC**C**TG**T**TA**T**CC**T**C-3′.

Neuronal stimulation

Neurons were treated with ASO or scrambled ASO (1 μM) for 18 hours prior to neuronal stimulation. To study activity-dependent gene regulation, neuronal cultures were treated with vehicle, 5 μM glutamate (10 minutes), or 35 mM KCl (5 minutes). After stimulation, cultures were washed with Hanks' buffered salt solution (HBSS, Thermo Fisher Scientific), and then replaced with fresh medium.

Quantitative RT-PCR analysis

Total RNA was isolated from primary cortical neurons or mouse hippocampus using TRI reagent (Sigma-Aldrich) according to the manufacturer's protocol. RNA concentration was measured using a NanoDrop ND-1000 spectrophotometer (Thermo Fisher Scientific). Total RNA was reverse transcribed using random decamers and M-MLV reverse transcriptase (Promega)/Superscript II RNase H reverse transcriptase (Thermo Fisher Scientific). Quantitative RT-PCR was performed on a BioRad CFX Connect system using iTaq Universal SYBR Green Supermix (BioRad). Designed primers were acquired from Integrated DNA Technologies and provided in Table S2. Desired amplicons were verified by melting curve analysis and followed by gel electrophoresis. The starting quantity of DNA from each sample was determined by interpolation of the threshold cycle (CT) from a standard curve of each primer set. Relative gene expression levels were normalized to the endogenous gene *GAPDH*.

Immunoblotting

Primary cortical neurons or mouse hippocampal tissues were lysed in RIPA lysis buffer with protease inhibitor (Santa Cruz Biotechnology). Crude synaptosomal fractions were prepared as previously described (Wirths, 2017). Protein concentrations were measured using bicinchoninic acid (BCA) protein assay (Thermo Fisher Scientific). Ten to 30 µg of protein samples were loaded on 10% sodium dodecyl sulfate polyacrylamide (SDS-PAGE) gels and separated by electrophoresis. Gels were electro-transferred onto polyvinylidene fluoride (PVDF) membranes using a semi-dry transfer system (BioRad). Membranes were either blocked with 5% nonfat milk or 5% bovine serum albumin

(BSA) in Tris-buffered saline/Tween 20 (0.1% [vol/vol]) (TBST) for 1 hour at room temperature. Membranes were incubated with primary antibodies overnight at 4 ºC. After primary antibody incubation, membranes were washed three times with TBST and then incubated with secondary antibodies for 1 hour at room temperature. Bands were detected using an enhanced chemiluminescence (ECL) kit (Thermo Fisher Scientific), visualized using BioRad Chemidoc MP imaging system, and analyzed by Image Lab software (BioRad). GAPDH was used as a loading control. All antibodies used in this study are listed in Table S3.

In vitro XTT cell viability assay

Primary cortical neurons (10,000 to 20,000 cells/well) were plated onto 96-well plates coated with poly-D-lysine. After 7–14 days, ASOs or scrambled ASOs were added and incubated for 18 hours. Cell viability was determined using the 2,3-bis[2-methoxy-4-nitro-5-sulfophenyl]-2H-tetrazolium-5-carboxyanilide inner salt (XTT) assay according to the manufacturer's protocol (Biotium). The assay utilizes the ability of viable cells with active metabolism to reduce the yellow tetrazolium salt to the soluble orange formazan product by mitochondrial dehydrogenase enzymes. The XTT reagent was added to each well and incubated for 2–4 hours at 37 °C and 5% CO_2. Absorbance was measured at 450 nm with a reference wavelength of 680 nm using a Biotek Synergy HT microplate reader. Results were normalized to control, and all samples were assayed in triplicate.

Stereotaxic surgeries

C57/BL6J mice (8–10 weeks old, Jackson Laboratory), housed under standard conditions with light-control (12-h light/12-h dark cycles), were anaesthetized with an isoflurane (1–3%)/oxygen vapor mixture. Mice were infused bilaterally to the CA1 region of the dorsal hippocampus with ribozyme ASO, scrambled ASO diluted in sterile PBS, or vehicle. The following coordinates were used, relative to bregma: medial-lateral (ML), ±1.5 mm; anterior-posterior (AP), −2.0 mm; dorsal-ventral (DV), −1.5 mm. ASOs or vehicle (1 nmol/μL) were infused bilaterally at a rate of 0.1 μL/min using a Neuros Hamilton syringe (Hamilton company) with a syringe pump (Harvard Apparatus). The injectors were left in place for 2 minutes to allow diffusion, and then were slowly removed at a rate of 0.1 mm per 15 sec. The incision site was sutured, and mice were allowed to recover on a warming pad and then were returned to cages. For all surgeries, mice were randomly assigned to the different conditions to avoid grouping same treatment conditions in time.

Object location memory (OLM) tasks

The OLM was performed to assess hippocampus-dependent memory, as previously described (Vogel-Ciernia and Wood, 2014). Briefly, naïve C57/BL6J mice (8–12 weeks old; n = 10–12/group; ribozyme ASO, scrambled ASO) were trained and tested. Prior to training, mice were handled 1–2 minutes for 5 days and then habituated to the experimental apparatus for 5 minutes on 6 consecutive days in the absence of objects. During training, mice were placed into the apparatus with two identical objects and allowed to explore the objects for 10 minutes. Twenty-four hours after training, mice were exposed to the same arena, and long-term memory was tested for 5 minutes, with

the two identical objects present, one of which was placed in a novel location. For all experiments, objects and locations were counterbalanced across all groups to reduce bias. Videos of training and testing sessions were analyzed for discrimination index (DI) and total exploration time of objects. The videos were scored by observers blind to the treatment. The exploration of the objects was scored when the mouse's snout was oriented toward the object within a distance of 1 cm or when the nose was touching the object. The relative exploration time was calculated as a discrimination index ($DI = (t_{novel} - t_{familiar}) / (t_{novel} + t_{familiar}) \times 100\%$). Mice that demonstrated a location or an object preference during the training trial (DI > ±20) were removed from analysis.

3′RACE

Total RNA was extracted from the mouse CA1 hippocampus. 3′ rapid amplification of cDNA ends (3′ RACE) was performed to study the alternative polyadenylation. cDNA was synthesized using oligo(dT) primers with 3′ RACE adapter primer sequence at the 5′ ends. This cDNA library results in a universal sequence at the 3′ end. A gene-specific primer (GSP) and an anchor primer that targets the poly(A) tail region were used for the first PCR using the following protocol: 95 °C for 3 minutes, followed by 30 cycles of 95 °C for 30 seconds, 55 °C for 30 seconds, and 72 °C for 3 minutes, with a final extension of 72 °C for 5 minutes. To improve specificity, a nested PCR was then carried out using primers internal to the first two primers. Upon amplification condition optimization, a quantitative PCR was performed on the first diluted PCR product using the nested primers, and a standard curve of the primer set was generated to determine the effect of relative expression of 3′-mRNA and alternative polyadenylation. All primers used in this

study are listed in Table S4. When resolved using agarose gel electrophoresis, this nested-primer qPCR produced single bands corresponding to the correct amplicons of individual cDNAs.

Quantification and statistical analysis

Data are presented as means ± SEM. Statistical analyses were performed using GraphPad Prism (GraphPad Prism Software). Statistical differences were determined using two-tailed Welch's *t* test when comparing between 2 independent groups, and one-way ANOVA with Sidak's *post hoc* tests when comparing across 3 or more independent groups. OLM data were analyzed with two-way ANOVA followed by Sidak's *post hoc* tests. $P < 0.05$ was considered significant.

Acknowledgments

We thank M. Malgowska , C-K. Lau, and M. A. Sta Maria for experimental assistance. This work was supported by NIH grants AG051807 and AG057558 to M.A.W., and NSF grants 1804220 and 1330606 to A.L. C.C.C. was supported by a National Science Foundation Graduate Research Fellowship (NSF GRFP).

References

Chadalavada, D.M., Gratton, E.A., and Bevilacqua, P.C. (2010). The human HDV-like CPEB3 ribozyme is intrinsically fast-reacting. Biochemistry-Us *49*, 5321-5330.

Chao, H.W., Lai, Y.T., Lu, Y.L., Lin, C.L., Mai, W., and Huang, Y.S. (2012). NMDAR signaling facilitates the IPO5-mediated nuclear import of CPEB3. Nucleic Acids Res *40*, 8484-8498.

Chao, H.W., Tsai, L.Y., Lu, Y.L., Lin, P.Y., Huang, W.H., Chou, H.J., Lu, W.H., Lin, H.C., Lee, P.T., and Huang, Y.S. (2013). Deletion of CPEB3 enhances hippocampus-dependent memory via increasing expressions of PSD95 and NMDA receptors. J Neurosci *33*, 17008-17022.

de la Pena, M., and Garcia-Robles, I. (2010). Intronic hammerhead ribozymes are ultraconserved in the human genome. Embo Rep *11*, 711-716.

Diering, G.H., and Huganir, R.L. (2018). The AMPA Receptor Code of Synaptic Plasticity. Neuron *100*, 314-329.

Drisaldi, B., Colnaghi, L., Fioriti, L., Rao, N., Myers, C., Snyder, A.M., Metzger, D.J., Tarasoff, J., Konstantinov, E., Fraser, P.E.*, et al.* (2015). SUMOylation Is an Inhibitory Constraint that Regulates the Prion-like Aggregation and Activity of CPEB3. Cell Rep *11*, 1694-1702.

Du, L., and Richter, J.D. (2005). Activity-dependent polyadenylation in neurons. RNA *11*, 1340-1347.

Eickbush, D.G., and Eickbush, T.H. (2010). R2 Retrotransposons Encode a Self-Cleaving Ribozyme for Processing from an rRNA Cotranscript. Molecular and Cellular Biology *30*, 3142-3150.

Fioriti, L., Myers, C., Huang, Y.Y., Li, X., Stephan, J.S., Trifilieff, P., Colnaghi, L., Kosmidis, S., Drisaldi, B., Pavlopoulos, E.*, et al.* (2015). The Persistence of Hippocampal-Based Memory Requires Protein Synthesis Mediated by the Prion-like Protein CPEB3. Neuron *86*, 1433-1448.

Fong, N., Ohman, M., and Bentley, D.L. (2009). Fast ribozyme cleavage releases transcripts from RNA polymerase II and aborts co-transcriptional pre-mRNA processing. Nat Struct Mol Biol *16*, 916-922.

Frey, U., and Morris, R.G.M. (1997). Synaptic tagging and long-term potentiation. Nature *385*, 533-536.

Gu, X.Y., Schafer, N.P., Wang, Q., Song, S.S., Chen, M.C., Waxham, M.N., and Wolynes, P.G. (2020). Exploring the F-actin/CPEB3 interaction and its possible role in the molecular mechanism of long-term memory. P Natl Acad Sci USA *117*, 22128-22134.

Hake, L.E., and Richter, J.D. (1994). CPEB is a specificity factor that mediates cytoplasmic polyadenylation during Xenopus oocyte maturation. Cell *79*, 617-627.

Harris, D.A., Tinsley, R.A., and Walter, N.G. (2004). Terbium-mediated footprinting probes a catalytic conformational switch in the antigenomic hepatitis delta virus ribozyme. J Mol Biol *341*, 389-403.

Hervas, R., Li, L.Y., Majumdar, A., Fernandez-Ramirez, M.D., Unruh, J.R., Slaughter, B.D., Galera-Prat, A., Santana, E., Suzuki, M., Nagai, Y.*, et al.* (2016). Molecular Basis of Orb2 Amyloidogenesis and Blockade of Memory Consolidation. Plos Biology *14*.

Hervas, R., Rau, M.J., Park, Y., Zhang, W., Murzin, A.G., Fitzpatrick, J.A.J., Scheres, S.H.W., and Si, K. (2020). Cryo-EM structure of a neuronal functional amyloid implicated in memory persistence in Drosophila. Science *367*, 1230-1234.

Hua, Y., Sahashi, K., Hung, G., Rigo, F., Passini, M.A., Bennett, C.F., and Krainer, A.R. (2010). Antisense correction of SMN2 splicing in the CNS rescues necrosis in a type III SMA mouse model. Genes Dev *24*, 1634-1644.

Huang, Y.S., Carson, J.H., Barbarese, E., and Richter, J.D. (2003). Facilitation of dendritic mRNA transport by CPEB. Genes Dev *17*, 638-653.

Huang, Y.S., Kan, M.C., Lin, C.L., and Richter, J.D. (2006). CPEB3 and CPEB4 in neurons: analysis of RNA-binding specificity and translational control of AMPA receptor GluR2 mRNA. Embo J *25*, 4865-4876.

Ivshina, M., Lasko, P., and Richter, J.D. (2014). Cytoplasmic polyadenylation element binding proteins in development, health, and disease. Annu Rev Cell Dev Biol *30*, 393-415.

Jimenez, R.M., Polanco, J.A., and Luptak, A. (2015). Chemistry and Biology of Self-Cleaving Ribozymes. Trends Biochem Sci *40*, 648-661.

Kandel, E.R. (2001). The molecular biology of memory storage: a dialogue between genes and synapses. Science *294*, 1030-1038.

Keleman, K., Kruttner, S., Alenius, M., and Dickson, B.J. (2007). Function of the Drosophila CPEB protein Orb2 in long-term courtship memory. Nat Neurosci *10*, 1587-1593.

Majumdar, A., Cesario, W.C., White-Grindley, E., Jiang, H., Ren, F., Khan, M.R., Li, L., Choi, E.M., Kannan, K., Guo, F.*, et al.* (2012). Critical role of amyloid-like oligomers of Drosophila Orb2 in the persistence of memory. Cell *148*, 515-529.

Martick, M., Horan, L.H., Noller, H.F., and Scott, W.G. (2008). A discontinuous hammerhead ribozyme embedded in a mammalian messenger RNA. Nature *454*, 899-U857.

Miniaci, M.C., Kim, J.H., Puthanveettil, S.V., Si, K., Zhu, H., Kandel, E.R., and Bailey, C.H. (2008). Sustained CPEB-dependent local protein synthesis is required to stabilize synaptic growth for persistence of long-term facilitation in Aplysia. Neuron *59*, 1024-1036.

Neugebauer, K.M. (2019). Nascent RNA and the Coordination of Splicing with Transcription. Csh Perspect Biol *11*.
Neves, G., Cooke, S.F., and Bliss, T.V. (2008). Synaptic plasticity, memory and the hippocampus: a neural network approach to causality. Nat Rev Neurosci *9*, 65-75.
Passalacqua, L.F.M., Jimenez, R.M., Fong, J.Y., and Luptak, A. (2017). Allosteric Modulation of the Faecalibacterium prausnitzii Hepatitis Delta Virus-like Ribozyme by Glucosamine 6-Phosphate: The Substrate of the Adjacent Gene Product. Biochemistry-Us *56*, 6006-6014.
Pavlopoulos, E., Trifilieff, P., Chevaleyre, V., Fioriti, L., Zairis, S., Pagano, A., Malleret, G., and Kandel, E.R. (2011). Neuralized1 activates CPEB3: a function for nonproteolytic ubiquitin in synaptic plasticity and memory storage. Cell *147*, 1369-1383.
Rayman, J.B., and Kandel, E.R. (2017). Functional Prions in the Brain. Cold Spring Harb Perspect Biol *9*.
Reimer, K.A., Mimoso, C., Adelman, K., and Neugebauer, K.M. (2020). Rapid and Efficient Co-Transcriptional Splicing Enhances Mammalian Gene Expression. bioRxiv.
Richter, J.D. (2007). CPEB: a life in translation. Trends Biochem Sci *32*, 279-285.
Richter, J.D. (2010). Translational control of synaptic plasticity. Biochem Soc T *38*, 1527-1530.
Ruminski, D.J., Webb, C.H., Riccitelli, N.J., and Luptak, A. (2011). Processing and translation initiation of non-long terminal repeat retrotransposons by hepatitis delta virus (HDV)-like self-cleaving ribozymes. J Biol Chem *286*, 41286-41295.
Salehi-Ashtiani, K., Luptak, A., Litovchick, A., and Szostak, J.W. (2006). A genomewide search for ribozymes reveals an HDV-like sequence in the human CPEB3 gene. Science *313*, 1788-1792.
Sanchez-Luque, F.J., Lopez, M.C., Macias, F., Alonso, C., and Thomas, M.C. (2011). Identification of an hepatitis delta virus-like ribozyme at the mRNA 5 '-end of the L1Tc retrotransposon from Trypanosoma cruzi. Nucleic Acids Research *39*, 8065-8077.
Seth, P.P., Siwkowski, A., Allerson, C.R., Vasquez, G., Lee, S., Prakash, T.P., Wancewicz, E.V., Witchell, D., and Swayze, E.E. (2009). Short antisense oligonucleotides with novel 2'-4' conformationaly restricted nucleoside analogues show improved potency without increased toxicity in animals. J Med Chem *52*, 10-13.
Sharmeen, L., Kuo, M.Y.P., Dintergottlieb, G., and Taylor, J. (1988). Antigenomic Rna of Human Hepatitis Delta-Virus Can Undergo Self-Cleavage. J Virol *62*, 2674-2679.
Si, K., Choi, Y.B., White-Grindley, E., Majumdar, A., and Kandel, E.R. (2010). Aplysia CPEB can form prion-like multimers in sensory neurons that contribute to long-term facilitation. Cell *140*, 421-435.
Si, K., Giustetto, M., Etkin, A., Hsu, R., Janisiewicz, A.M., Miniaci, M.C., Kim, J.H., Zhu, H., and Kandel, E.R. (2003). A neuronal isoform of CPEB regulates local protein

synthesis and stabilizes synapse-specific long-term facilitation in aplysia. Cell *115*, 893-904.
Si, K., and Kandel, E.R. (2016). The Role of Functional Prion-Like Proteins in the Persistence of Memory. Cold Spring Harb Perspect Biol *8*, a021774.
Singh, J., and Padgett, R.A. (2009). Rates of in situ transcription and splicing in large human genes. Nat Struct Mol Biol *16*, 1128-1133.
Skilandat, M., Rowinska-Zyrek, M., and Sigel, R.K. (2016). Secondary structure confirmation and localization of Mg2+ ions in the mammalian CPEB3 ribozyme. RNA *22*, 750-763.
Stephan, J.S., Fioriti, L., Lamba, N., Colnaghi, L., Karl, K., Derkatch, I.L., and Kandel, E.R. (2015). The CPEB3 Protein Is a Functional Prion that Interacts with the Actin Cytoskeleton. Cell Rep *11*, 1772-1785.
Theis, M., Si, K., and Kandel, E.R. (2003). Two previously undescribed members of the mouse CPEB family of genes and their inducible expression in the principal cell layers of the hippocampus. Proc Natl Acad Sci U S A *100*, 9602-9607.
Vogel-Ciernia, A., and Wood, M.A. (2014). Examining object location and object recognition memory in mice. Curr Protoc Neurosci *69*, 8 31 31-17.
Vogler, C., Spalek, K., Aerni, A., Demougin, P., Muller, A., Huynh, K.D., Papassotiropoulos, A., and de Quervain, D.J. (2009). CPEB3 is associated with human episodic memory. Front Behav Neurosci *3*, 4.
Webb, C.H., and Luptak, A. (2011). HDV-like self-cleaving ribozymes. RNA Biol *8*, 719-727.
Webb, C.H., Riccitelli, N.J., Ruminski, D.J., and Luptak, A. (2009). Widespread occurrence of self-cleaving ribozymes. Science *326*, 953.
Wirths, O. (2017). Preparation of Crude Synaptosomal Fractions from Mouse Brains and Spinal Cords. Bio-Protocol *7*.
Wu, H.N., Lin, Y.J., Lin, F.P., Makino, S., Chang, M.F., and Lai, M.M.C. (1989). Human Hepatitis-Delta Virus-Rna Subfragments Contain an Autocleavage Activity. P Natl Acad Sci USA *86*, 1831-1835.

Figures

Figure 1.

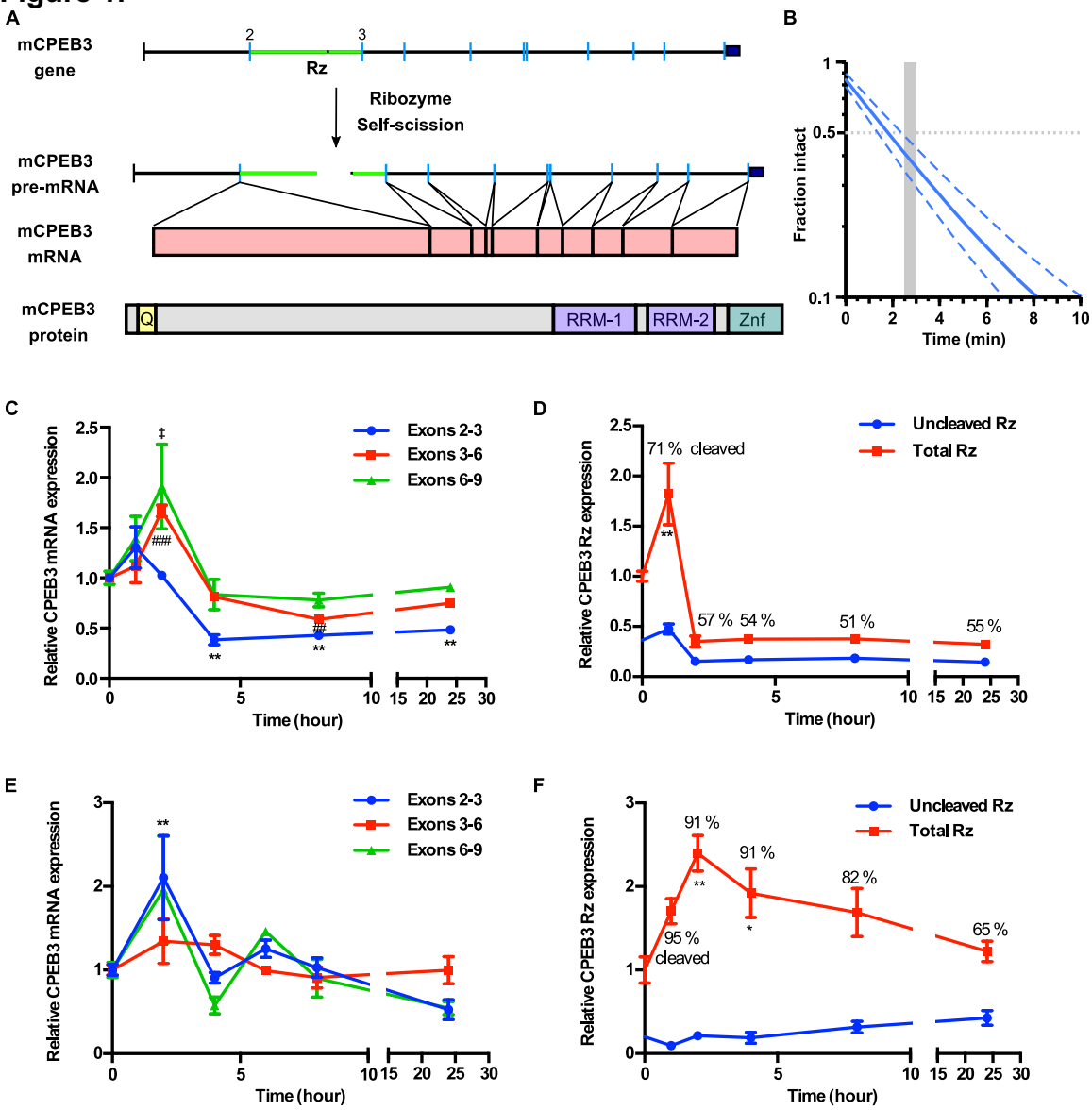

Figure 1. CPEB3 ribozyme activity and its effect on primary cortical neurons. (A) Schematic representation of mouse *CPEB3* gene and its products. Rz denotes the ribozyme location in the 2nd intron (green) between the 2nd and 3rd exons. Co-transcriptional self-scission is shown by a break in the pre-mRNA 2nd intron. Fully-spliced mRNA is shown independent of the ribozyme activity. (B) Co-transcriptional self-

cleavage activity of a 470-nt construct, incorporating the 72-nt ribozyme, which cuts the transcript 233 nts from the 5′ terminus (see table S1 for kinetic parameters of this and other constructs). Log-linear graph of self-cleavage is shown with solid blue line (dashed lines show ± standard deviation). Gray dotted line indicates mid-point of self-cleavage (with resulting $t_{1/2}$ of ~2 minutes). Gray bar indicates the approximate time range for RNAPII to reach from the ribozyme to the 3rd exon, at which point ~40% of the intron would remain intact. (C) KCl stimulation profile of the *CPEB3* gene showing induction of spliced CPEB3 exons (one-way ANOVA with Sidak's *post hoc* tests. $^{*}P < 0.05$, $^{**}P < 0.01$, $\#\#P < 0.01$, $\#\#\#P < 0.001$, ‡$P < 0.05$). (D) KCl stimulation profile of CPEB3 ribozyme expression (uncleaved and total). Cleaved ribozyme fraction is calculated as [(total ribozyme – uncleaved ribozyme)/total ribozyme] and shown as % cleaved. (E) Expression of CPEB3 mRNA exons 2–3 is upregulated 2 hours after glutamate stimulation (one-way ANOVA with Sidak's multiple comparisons *post hoc* test. $^{**}P < 0.01$). (F) Glutamate stimulation induces an increase in CPEB3 ribozyme levels at 2-hour time point (one-way ANOVA with Sidak's multiple comparisons *post hoc* test. $^{*}P < 0.05$, $^{**}P < 0.01$). Data are presented as mean ± SEM.

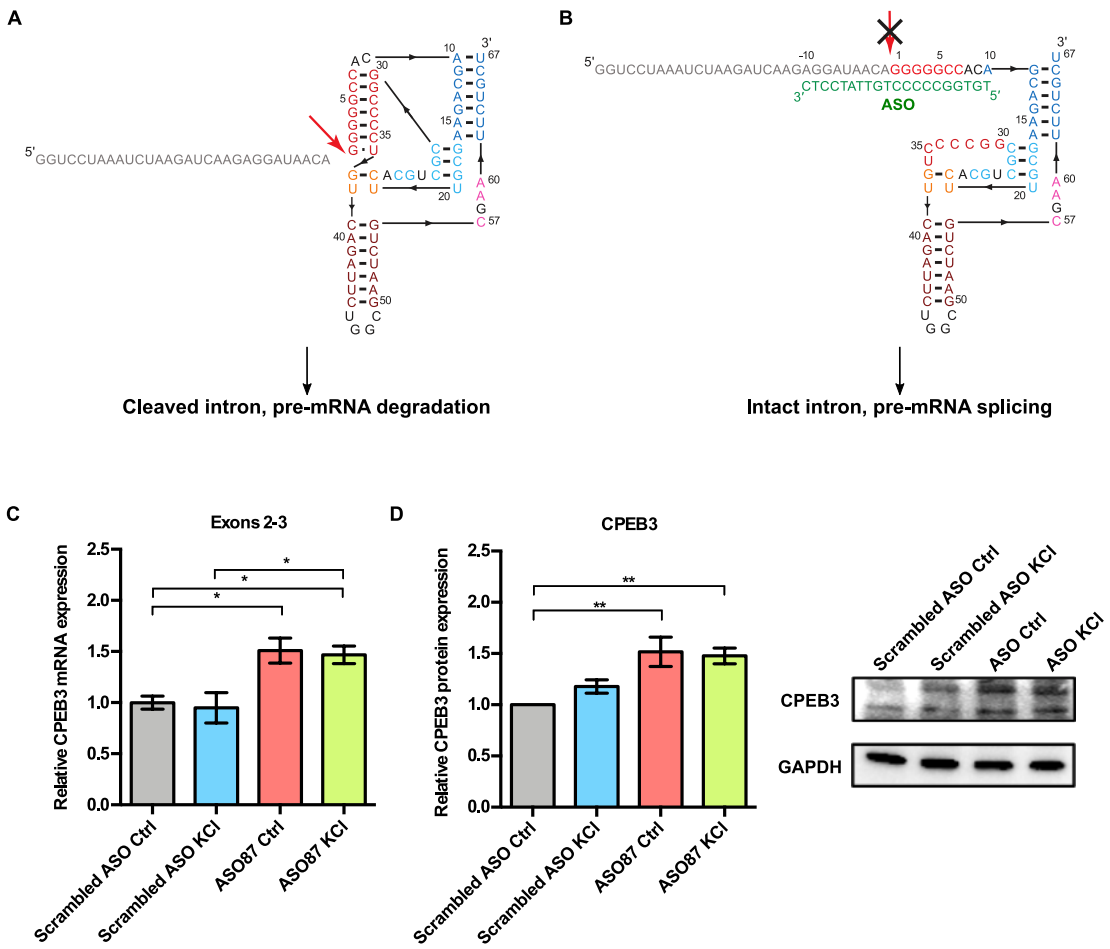

Figure 2. CPEB3 mRNA and protein are upregulated in primary neuronal cultures treated with ASO.

(A) Inhibition of the CPEB3 ribozyme by an ASO targeting its cleavage site. Secondary structure of the ribozyme (colored by structural elements (Webb and Luptak, 2011)). Sequence upstream of the ribozyme is shown in gray, and the site of self-scission is shown with the red arrow. (B) Model of the ribozyme inhibited by the antisense oligonucleotide (ASO, green letters) showing base-pairing between the ASO and 10 nts upstream and downstream of the ribozyme cleavage site. Inhibition of self-scission is indicated by crossed arrow. (C) Ribozyme inhibition by ASO in cultured cortical neurons

resulted in upregulation of CPEB3 mRNA (exons 2–3; one-way ANOVA with Sidak's *post hoc* tests, $*P < 0.05$). (D) Effect of CPEB3 ribozyme ASO on CPEB3 protein expression. GAPDH is used as a loading control (one-way ANOVA with Sidak's *post hoc* tests, $*P < 0.05$, $**P < 0.01$). Data are presented as mean ± SEM.

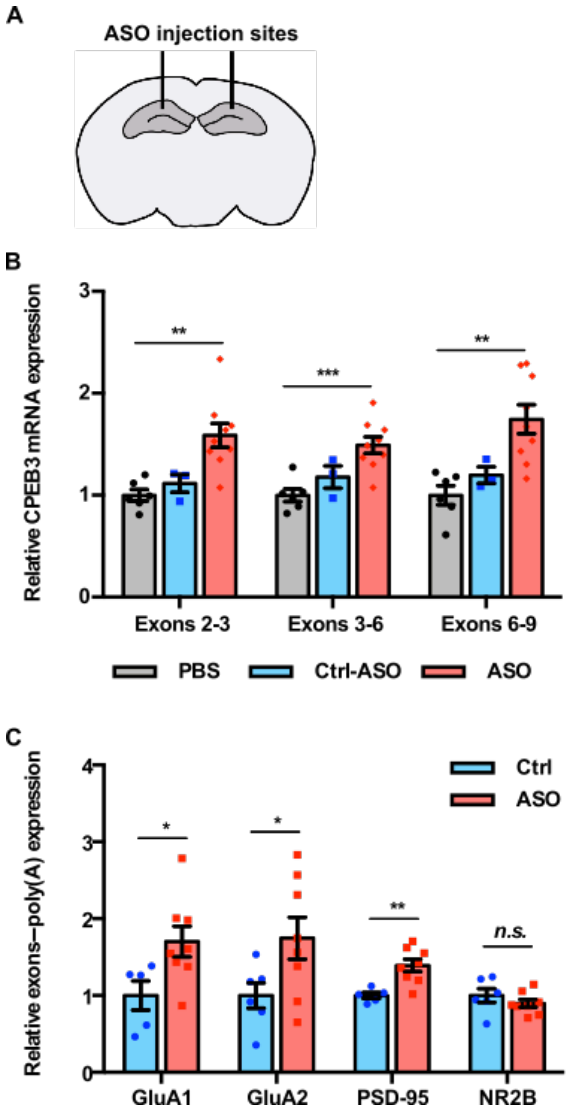

Figure 3. CPEB3 ribozyme ASO leads to an increase of CPEB3 mRNA and polyadenylation of PRPs in the CA1 hippocampus.

(A) Schematic representation of stereotaxic procedure. ASO, scrambled ASO, or vehicle was bilaterally infused to the mouse CA1 hippocampus. (B) CPEB3 mRNA expression is upregulated in the CPEB3 ribozyme ASO treatment group compared to controls (one-way ANOVA with Sidak's *post hoc* tests. $^{**}P < 0.01$, $^{***}P < 0.001$). (C) Inhibition of CPEB3 ribozyme results in increased polyadenylation of plasticity-related

genes (unpaired *t* test, *$P < 0.05$, **$P < 0.01$, *n.s.* not significant). Data are presented as mean ± SEM.

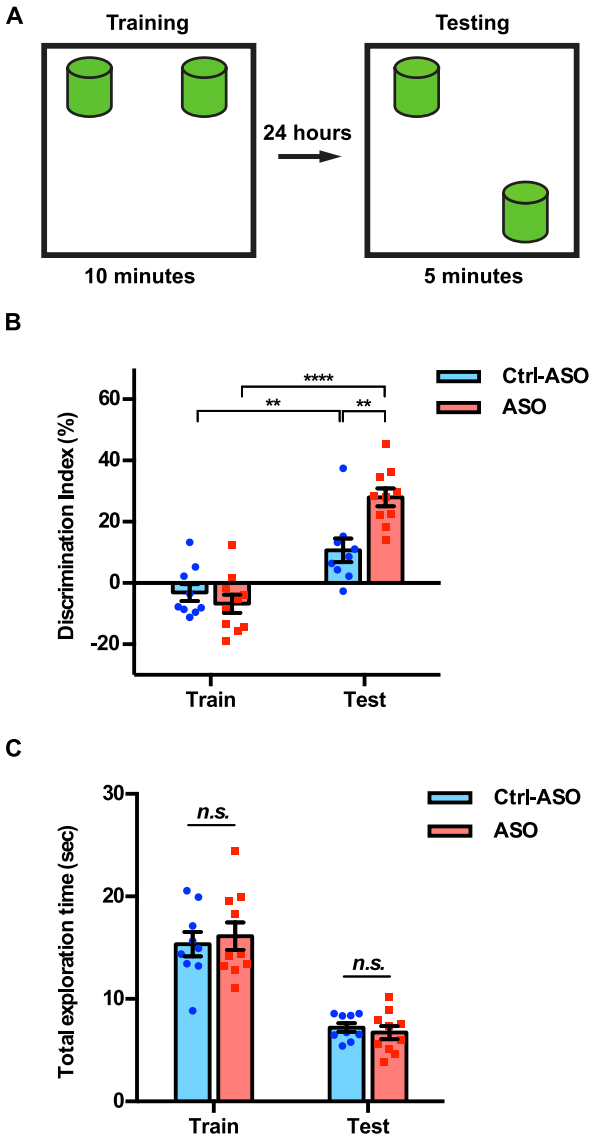

Figure 4. Inhibition of CPEB3 ribozyme enhances long-term OLM.

(A) Experimental procedure testing long-term memory. (B) Mice infused with CPEB3 ribozyme ASO show significant discrimination index in OLM testing (two-way ANOVA with Sidak's *post hoc* tests, $*P < 0.05$, $**P < 0.01$, $****P < 0.0001$). (C) CPEB3 ribozyme ASO and control mice display similar total exploration time (one-way ANOVA with Sidak's *post hoc* tests, *n.s.* not significant). Data are presented as mean ± SEM.

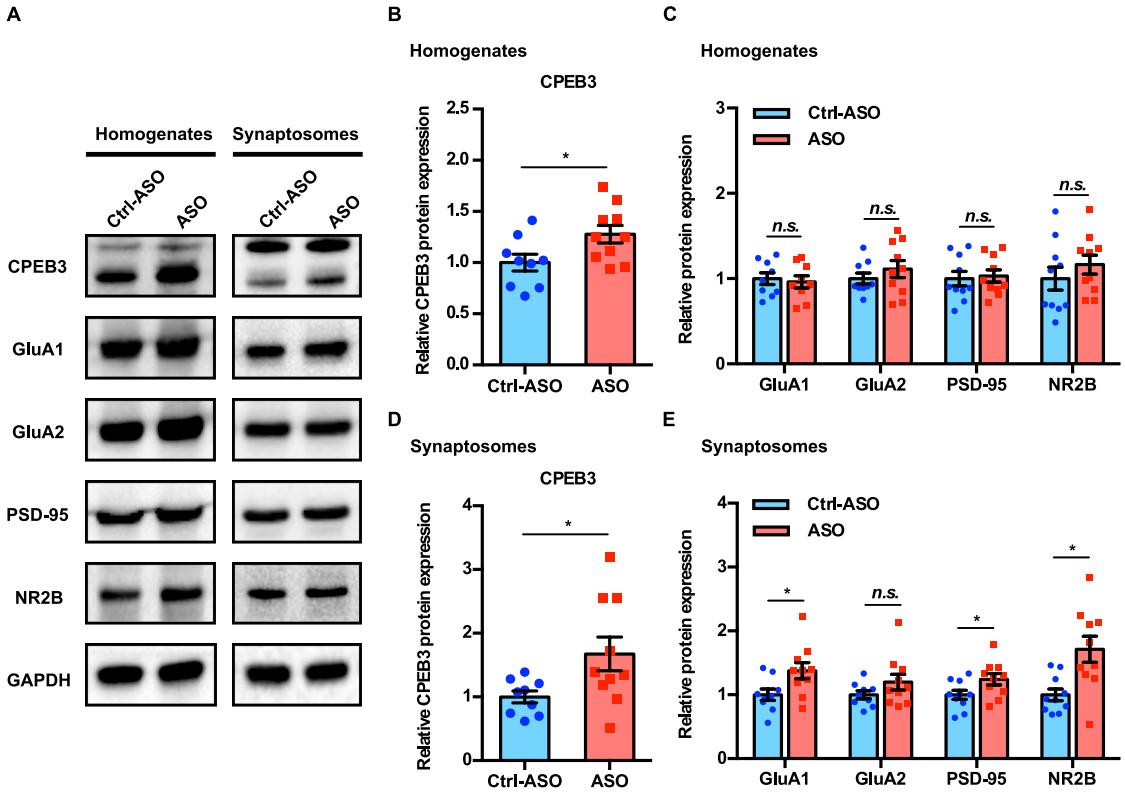

Figure 5. Inhibition of CPEB3 ribozyme leads to upregulation of CPEB3 and PRPs protein expression after OLM.

(A) Representative images of immunoblotting analysis. GAPDH is used as a loading control. Quantification of CPEB3 (B) and PRPs (C) in tissue homogenates shows increased CPEB3, but not PRPs, protein expression (unpaired *t* test, $^*P < 0.05$, *n.s.* not significant). (D) In synaptosomes, the protein expression of both CPEB3 (D) and PRPs (E) is increased (unpaired *t* test, $^*P < 0.05$, *n.s.* not significant). Data are presented as mean ± SEM.